Artificial Neural Network Modeling of Distillers Dried Grains with Solubles (DDGS) Flowability with Varying Process and Storage Parameters

Rumela Bhadra,[1] K. Muthukumarappan,[1] and Kurt A. Rosentrater[2,3]

Cereal Chem. 88(5):480–489

ABSTRACT

Neural network (NN) modeling techniques were used to predict flowability behavior of distillers dried grains with solubles (DDGS) prepared with varying levels of condensed distillers solubles (10, 15, and 20%, wb), drying temperatures (100, 200, and 300°C), cooling temperatures (–12, 25, and 35°C), and storage times (0 and 1 month). Response variables were selected based on our previous research results and included aerated bulk density, Hausner ratio, angle of repose, total flowability index, and Jenike flow index. Various NN models were developed using multiple input variables in order to predict single-response and multiple-response variables simultaneously. The NN models were compared based on R^2, mean square error, and coefficient of variation obtained. In order to achieve results with higher R^2 and lower error, the number of neurons in each hidden layer, the step size, the momentum learning rate, and the number of hidden layers were varied. Results indicate that for all the response variables, $R^2 > 0.83$ was obtained from NN modeling. Compared with our previous studies, NN modeling provided better results than either partial least squares modeling or regression modeling, indicating greater robustness in the NN models. Surface plots based on the predicted values from the NN models yielded process and storage conditions for favorable versus cohesive flow behavior for DDGS. Modeling of DDGS flowability using NN has not been done before, so this work will be a step toward the application of intelligent modeling procedures to this industrial challenge.

Because fossil fuels are not replenishable, the global population is becoming more aware of the need to use alternative renewable energy sources and to develop greener sources of fuel. Bioethanol has become a major source of alternative fuel during the past decade. The U.S. fuel ethanol industry has shown remarkable growth in the past few years, and it is estimated that by 2015, U.S. ethanol production will exceed 15×10^9 gal/year (56.77×10^9 L/year) (Denicoff 2007). Distillers dried grains with solubles (DDGS) is the primary coproduct from the corn-based ethanol industry, and it has high market demand as livestock feed for ruminants and nonruminants.

DDGS is produced by mixing distillers wet grains (DWG) (containing nonfermentable solids) and condensed distillers solubles (referred to as CDS or "syrup" in the industry), which is produced by centrifuging the whole stillage after fermentation and evaporating the centrifuge stream. After the DWG and CDS are combined, the mixture is then subjected to drying at high temperatures, often having 1000°F inlet and 300°F outlet temperatures (Bhadra et al *in press* b). The resultant golden-brown powder or bulk solid is called DDGS. After drying, the DDGS is often placed in piles in flat storage buildings to cool under ambient conditions.

The drying process forms an integral part of DDGS production, and it affects the flow behavior and physical and chemical properties of the DDGS. Precise drying and cooling conditions for DDGS are not standardized in the industry, however, and there is much variability in this process among ethanol plants. However, the final moisture content of DDGS is often targeted to be 5–10% (dry basis, db) (Bhadra et al *in press* b).

DDGS is an excellent source of protein (≈32%, db), fiber (≈35%, db), and fat (≈10%, db) (Bhadra et al 2010b) and an important source of vitamins and minerals for livestock feed. With the rapid growth in the ethanol industry, the production of DDGS has also increased. It is reported that more than 30 million metric tons of DDGS was produced in the United States in 2010 (RFA 2010). Thus, increasing the effective use of this product in domestic and international markets is important to the ethanol industry. DDGS is mostly transported in rail cars or trucks and is even shipped overseas by barge or container. DDGS can be subjected to diverse environmental conditions (such as variations in temperature, humidity, and amount of vibration) and can harden and agglomerate during transport and shipping. Agglomeration, stickiness, and caking of DDGS particles during transport cause unwanted flow problems, which are a major economic concern to the industry because of fines, costs, and labor involved in unloading (AURI and MCGA 2005). Thus, understanding the flow behavior of DDGS under diverse environmental and processing conditions is important for improving handling and storage operations.

Reliable flow of granular solids from storage vessels is a major concern in the agricultural, food and dairy, mineral and mining, and pharmaceutical industries. A thorough knowledge of powder flow is necessary for developing processing and handling techniques, including storage, flow from hoppers and silos, transportation, mixing, drying, compressing, packaging, and other operations (Knowlton et al 1994). Industrial bulk solids are generally cohesive, and thus physical and flowability properties will determine whether the mass will compress, mix, segregate, cake, or flow out of hoppers (Faqih et al 2007). Design and operation of unit operations depend on flowability (Santomaso et al 2003). Despite advances in characterizing and quantifying the flow behavior of cohesive systems, flow behavior tends to be poorly understood (Faqih et al 2007). Developing numerical models of flowability using empirical data is needed.

Neural network (NN), also known as artificial neural network (ANN), analysis is a powerful tool for data modeling (Batchelor et al 1997; Kachrimanis et al 2003; Baawain et al 2007; Marini et al 2007; Ochoa-Martinez et al 2007; Sofu and Ekinci 2007; Olajos et al 2008; Riahi et al 2008). NN is a type of computer-algorithm architecture that is able to relate inputs and outputs through training, or of learning through iteration, even though no prior knowledge about the relationships between input and output parameters exists. The main advantages of NN are that it is able to adapt to a new or changed environment, to calculate faster, and to model unlearned data (Torrecilla et al 2005). NN models consist of an input layer, a hidden layer, and an output layer that can arbitrarily provide accurate approximations by utilizing an adequate number of hidden layers (Olajos et al 2008). NN modeling is based on the human brain structure, with neurons containing a weight factor (produced by the transfer function used) for each of the inputs (Olajos et al 2008). Evi-

[1] Graduate research assistant and professor, respectively. Department of Agricultural and Biosystems Engineering, South Dakota State University, Brookings, SD.
[2] Assistant professor, Department of Agricultural and Biosystems Engineering, Iowa State University, Ames, IA.
[3] Corresponding author. Phone: 515-294-4019. Fax: 515-294-6633. E-mail: karosent@iastate.edu

doi:10.1094/CCHEM-12-10-0179

dence has shown that NN can work well for cases in which there are inconsistencies or noise in the dataset (Biollereaux et al 2003). Because NN models are developed through learning by iteration and adaptive training, it is expected that these models will lead to more robust predictive models, with multiple input variables obtained from multiple sets of experiments, as compared with regression modeling. For example, Linko et al (1992), Ganjyal et al (2006), and Chevanan et al (2007) used NN modeling for food extrusion processing and proved that NN modeling techniques resulted in better models than did nonlinear regression.

Regression modeling is commonly used for predicting relationships between input and output variables. Most regression modeling is done using either linear or nonlinear models and can yield higher-order terms and cross-products. But higher-order interaction terms and a large number of cross-products in the models may lead to large error terms when there is actually less variation in the data. Thus, sometimes regression modeling can increase the chance of an incorrect prediction (Chevanan et al 2007).

With respect to modeling the flow properties of powders, several attempts have been made over the years. Mikami et al (1998) and McCarthy et al (2001) modeled cohesion phenomena resulting from moisture in powders. Yang and Hsiau (2001) developed simulation models for liquid bridge strength in a vibrated bed of wet glass beads. Weir (2004) modeled the flow of noncohesive powders in steep-wall hoppers with variable density. McCarthy and Ottino (1998) used discrete element modeling to simulate flow in rotating drums. Faqih et al (2007) simulated the dynamic behavior of cohesive and noncohesive powders in a rotating drum.

Several studies dealing specifically with DDGS flowability have examined the Carr (1965) and Jenike (1964) properties using varying experimental variables, such as soluble solid and moisture content levels (Ganesan et al 2007, 2008a), as well as CDS, drying temperature, and cooling temperature levels (Bhadra et al 2010a, 2010c). Further, moisture content, water activity, and specific weight are properties that can indirectly measure the flowability of powders (Ilari 2002). In terms of modeling the flowability of DDGS, data mining techniques and nonlinear regression modeling have been used before. A study by Ganesan et al (2007) yielded flowability plots with $R^2 > 0.90$, and Bhadra et al (2010c) developed models with $R^2 > 0.70$ for predicting DDGS flowability with varying process and storage variables. However, DDGS flow modeling using NN techniques has not been examined yet. NN is a powerful modeling tool, and the application of NN techniques for modeling DDGS flowability would be an essential step forward.

Thus, the objective of this study was to model DDGS flowability via NN by selecting several key flow properties, including angle of repose (AoR), Hausner ratio (HR), aerated bulk density (ABD), Carr compressibility (CC), total flowability index (TFI), and Jenike flow index (JFI). The DDGS samples were prepared under laboratory conditions with different levels of process variables (CDS and drying temperature) and storage variables (cooling temperature and storage time), as described in Bhadra et al (2010a). The best NN models were then compared with results obtained from other studies, specifically partial least squares (PLS) modeling (Bhadra et al 2010a), and then our optimal models were validated with previous data, specifically the DDGS flow property dataset of Ganesan et al (2007). This paper will provide a step toward understanding DDGS flow using intelligence-based modeling tools.

MATERIALS AND METHODS

Data Pooling and Compilation

Data for Carr (1965) and Jenike (1964) shear test flow properties were obtained from our previous study (Bhadra et al 2010a) and then compiled with new flow data for samples stored for one month (data not published). DDGS samples were prepared in the laboratory with multiple CDS levels (10, 15, and 20%, wb) and drying temperatures (100, 200, and 300°C) and then cooled at varying cooling temperatures (–12, 25, and 35°C). DWG samples collected from a commercial ethanol plant were mixed with the appropriate CDS levels (also procured from the same ethanol plant). Drying was done for about 60 min (100°C), 30 min (200°C), or 10 min (300°C) in a conventional laboratory oven so that the final DDGS moisture content for all samples was 8% (db), which is close to industry practice. Details on drying equipment and procedures can be found in Bhadra et al (2010a). The drying temperature, CDS, and cooling temperature ranges used in this study were based on Bhadra et al (2010a) and on interviews with industry experts. A second set of samples, prepared with similar CDS, drying temperature, and cooling temperature levels, were stored for one month after production, and then Carr and Jenike shear

TABLE I
Independent and Dependent (Response) Variables Used for the Neural Network Modeling in This Study

Independent Variables	Level		
Condensed distillers solubles (%, wb)	10	15	20
Drying temperature (°C)	100	200	300
Cooling temperature (°C)	–12	25	35
Storage time (month)	0		1
Dependent (Response) Variables	**Units**		
Angle of repose	°		
Hausner ratio	-		
Aerated bulk density	g/cm^3		
Carr compressibility	%		
Total flowability index	-		
Jenike flow index	-		

TABLE II
Experimental Design Used in This Study, Based on Taguchi's Orthogonal Array (L_{27}), to Examine Various Neural Network Structures[a]

Trial	PE	Step Size (Hidden Layer)	Mom Rate (Hidden Layer)	Step Size (Output Layer)	Mom Rate (Output Layer)
1	4	0.10	0.30	0.10	0.30
2	4	0.10	0.30	0.10	0.50
3	4	0.10	0.30	0.10	0.70
4	4	1.00	0.50	1.00	0.30
5	4	1.00	0.50	1.00	0.50
6	4	1.00	0.50	1.00	0.70
7	4	2.00	0.70	2.00	0.30
8	4	2.00	0.70	2.00	0.50
9	4	2.00	0.70	2.00	0.70
10	8	0.10	0.50	2.00	0.30
11	8	0.10	0.50	2.00	0.50
12	8	0.10	0.50	2.00	0.70
13	8	1.00	0.70	0.10	0.30
14	8	1.00	0.70	0.10	0.50
15	8	1.00	0.70	0.10	0.70
16	8	2.00	0.30	1.00	0.30
17	8	2.00	0.30	1.00	0.50
18	8	2.00	0.30	1.00	0.70
19	12	0.10	0.70	1.00	0.30
20	12	0.10	0.70	1.00	0.50
21	12	0.10	0.70	1.00	0.70
22	12	1.00	0.30	2.00	0.30
23	12	1.00	0.30	2.00	0.50
24	12	1.00	0.30	2.00	0.70
25	12	2.00	0.50	1.00	0.30
26	12	2.00	0.50	1.00	0.50
27	12	2.00	0.50	1.00	0.70

[a] PE = number of processing elements; Mom Rate = momentum learning rate; one hidden layer was used for all trials.

test properties were measured. Thus, there were four independent variables (CDS, drying temperature, cooling temperature, and storage time) in the combined data set. Cooling temperature and storage time were the "storage" variables for this paper. Carr and Jenike shear flow properties, including AoR, HR, ABD, CC, TFI, and JFI, were selected as the response (dependent) variables for the NN modeling. Details for all of the Carr test procedures and properties can be found in Carr (1965) and Bhadra et al (2009a). Similarly, details of Jenike shear test procedures and properties can be found in Jenike (1964) and Bhadra et al (2009a). The list of independent and dependent (response) variables is given in Table I.

Experimental Design and Network Parameter Selection

One challenge of this study was in selecting appropriate network parameters for the modeling process. According to Chevanan et al (2007), a generalized feed-forward architecture, momentum rate from 0.2 to 0.7, initial step size from 0.1 to 0.3, one hidden layer, and default decay weight of 0.01 yielded models with high R^2 for modeling of extruded feed properties. Also, it has been recommended by commercial software (Neurodimensions, Gainesville, FL) to use one hidden layer and a multilayer perception (MLP) network in the beginning. Hence, based on Chevanan et al (2007) and software recommendations, we carried out some preliminary trials for modeling using Neurosolutions version 6 (Neurodimensions). On the basis of several preliminary trials (data not shown), we found that for hidden and output layers, processing elements from 4 to 12, step sizes from 0.1 to 2.0, and momentum rates from 0.3 to 0.7 yielded high R^2 and low coefficients of variation (CV). However, in the output layer, the number of processing elements was not varied and was kept at the default values (depending on the given network structure) generated by the software itself.

For all models, we used 70% of the data to generate the models, the training set held 10% of the data for cross-validation (or stopping criteria), and the testing set held 20% of the data. The data were allocated randomly. Each of the models was trained for three times with standard training steps of 1,000 epochs, using a supervised learning process. The TanhAxon transfer function was used for all trials. This procedure incorporates a layer of processing elements with hyperbolic nonlinear transfer functions, and the output range is from –1 to 1. Also, we used MLP network architecture for all the trials; MLP is considered the most widely used NN for general classification and regression. MLP feed-forward networks are typically trained with a static back-propagation algorithm. The main advantage is that they are easy to use and can approximate any input-output maps. All NN modeling trials were done with one hidden layer because more than one hidden layer may lead to the problem of local minima (Ochoa-Martinez et al 2007).

We developed a formal experimental design based on our preliminary trials, one that would vary each of the network parameters. We used a Taguchi orthogonal array (L_{27}) with five network variables, including number of processing elements (hidden layer), step size (hidden layer), momentum rate (hidden layer), step size (output layer), and momentum rate (output layer). For these five variables, we used an equidistant three-level design, which yielded the L_{27} orthogonal array. The experimental design is given in Table II. This design was used to develop models for each dependent variable with multiple inputs and single output, in which a single response variable was a function of all independent variables. The results of the best NN model for each response variable were then compared with the results of PLS modeling obtained from Bhadra et al (2010a). The DDGS flowability dataset obtained from Ganesan et al (2007) was then used to validate the optimal NN model parameters. Finally, through TableCurve 3D software (version 4.0.01, SYSTAT Software, San Jose, CA), the predicted values of flow properties obtained from the optimal NN modeling output were graphically displayed against varying CDS levels and the ratio of cooling temperature to drying temperature (C/D).

TABLE III
Neural Network Modeling Output for Angle of Repose (AoR), Hausner Ratio (HR), and Aerated Bulk Density (ABD) with Multiple Input Single Output[a]

	AoR			HR			ABD		
Trial	R^2	MSE	CV (%)	R^2	MSE	CV (%)	R^2	MSE	CV (%)
1	0.75	2.33	2.76	0.09	0.005	4.16	0.40	0.0005	4.02
2	0.75	2.29	2.66	0.30	0.005	5.00	0.57	0.0004	3.48
3	0.76	2.18	2.54	0.30	0.005	4.04	0.55	0.0004	3.56
4	0.71	2.46	2.85	0.20	0.005	4.41	0.55	0.0004	3.64
5	0.73	2.39	2.83	0.38	0.011	6.46	0.56	0.0004	3.63
6	0.73	2.35	0.48	0.68	0.002	3.27	0.57	0.0004	3.41
7	0.75	2.22	2.64	0.65	0.005	3.09	0.46	0.0005	3.88
8	0.81	2.04	2.47	0.64	0.005	3.13	0.54	0.0004	3.61
9	0.77	2.09	2.49	0.63	0.005	3.86	0.50	0.0004	3.69
10	0.75	2.24	2.66	0.48	0.005	4.13	0.57	0.0004	3.58
11	0.76	2.17	2.60	0.51	0.004	3.57	0.53	0.0004	3.71
12	0.79	2.05	2.55	0.32	0.004	3.30	0.52	0.0004	3.71
13	0.75	2.25	2.60	0.46	0.006	4.40	0.57	0.0004	3.48
14	0.76	2.20	2.60	0.39	0.005	3.76	0.57	0.0004	3.51
15	0.75	2.26	2.48	0.68	0.005	3.12	0.58	0.0004	3.56
16	**0.87**	**1.69**	**2.16**	0.42	0.003	3.44	0.57	0.0004	3.41
17	0.79	1.97	2.47	0.36	0.005	3.82	**0.83**	**0.0004**	**3.32**
18	0.76	2.19	2.57	0.65	0.003	3.40	0.55	0.0004	3.60
19	0.76	2.19	2.59	0.29	0.005	3.79	0.59	0.0004	3.50
20	0.77	2.11	2.65	0.61	0.004	3.69	0.59	0.0004	3.46
21	0.78	2.02	2.60	0.41	0.01	4.70	0.54	0.0004	3.63
22	0.74	2.25	2.68	0.66	0.002	3.28	0.49	0.0004	0.48
23	0.80	1.79	2.44	0.76	0.003	3.77	0.51	0.0005	3.75
24	0.78	1.88	2.39	0.46	0.006	4.38	0.58	0.0004	3.53
25	0.77	2.09	2.57	0.25	0.004	4.00	0.59	0.0004	3.48
26	0.78	1.93	2.39	**0.84**	**0.002**	**2.30**	0.57	0.0003	3.50
27	0.77	2.05	2.42	0.78	0.004	3.83	0.60	0.0004	3.51

[a] R^2 = coefficient of determination; MSE = mean square error; and CV = coefficient of variation. Bold font indicates that this neural network combination was best for modeling the response variable.

RESULTS AND DISCUSSION

NN Models

Tables III and IV present the modeling output for each response variable (listed in Table I), with CDS (%, wb), drying temperature (°C), cooling temperature (°C), and storage time (months) as the independent variables. For each dependent variable, the best model and its corresponding network architecture was chosen based on highest R^2, lowest CV value, and low MSE (mean square error). From Table III, for AoR, trial 16 (eight processing elements) yielded the best model (R^2 = 0.87, CV = 2.16%, MSE = 1.69). For HR, trial 26 (12 processing elements) yielded the best model (R^2 = 0.84, CV = 2.30%). For ABD, trial 17 (eight processing elements) yielded the best model (R^2 = 0.83, CV = 3.32%). From Table IV, for CC, trial 26 (12 processing elements) yielded the best model (R^2 = 0.86, CV = 15.05%); even though trial 21 yielded 13.79% CV, it was not selected as the best model because of its lower R^2 (0.74). For TFI, trial 26 (12 processing elements) yielded the best model (R^2 = 0.87, CV = 1.22%, MSE = 1.31). For JFI, trial 4 (four processing elements) yielded the best model (R^2 = 0.83, CV = 23.50%, MSE = 0.96). Except for CC and JFI, the CV values were below 10%, indicating that the NN models were a good fit with observed values. Chevanan et al (2007) also showed mixed results; for some of the response variables, CV was below 10%, and for other variables the CV ranges were higher (≈15%). For Chevanan et al (2007), increasing the number of input variables increased the R^2, decreased CV, and provided better accuracy for predicted models. However, for the current study, such behavior did not occur.

Figure 1 is the graphical representation of the optimal NN model performance for all response variables in Table I (with CDS, drying temperature, cooling temperature, and storage time as the independent variables). AoR, HR, ABD, and TFI showed good fit between observed (solid line) and predicted (dashed line) values for every exemplar. Exemplar is a complete pattern of samples in NN modeling, and it is related to the number of independent variables. It was calculated as the total number of data points in the input file divided by the number of processing elements. For CC, there was some scatter between observed and predicted values for exemplars 1 and 4; however, the rest of the graph showed close resemblances between observed and predicted values. On the other hand, the JFI and TFI/JFI graphs showed differences between observed and predicted values. Figure 2 is the graphical representation of AoR, JFI, TFI/JFI, and HR NN models, but without storage time as one of the independent variables (this was done to subsequently compare PLS model results with those of Bhadra et al (2010a), which did not use storage time as a factor). From Figure 2, it is noted that for AoR, TFI/JFI, and HR, the NN models yielded a good fit between observed (solid line) and predicted (dashed line) plots.

Moving a step further, with the best NN model combinations obtained for each of the dependent variables, we compared results with PLS multivariate modeling results obtained from our previous study (Bhadra et al 2010a), which had the same CDS, drying temperature, and cooling temperature levels. In order to have an ideal comparison between NN and PLS, we did not include storage time as an independent variable, because in Bhadra et al (2010a) storage time was not part of that study. Table V represents the comparison of NN modeling with PLS modeling results obtained from Bhadra et al (2010a). AoR yielded R^2 = 0.89 for both NN and PLS modeling; however, PLS modeling required nine principal components to build the model, indicating a complex multidimensional network. Thus, the NN procedure yielded a better model for AoR. JFI yielded lower R^2 (0.73) compared with the PLS model (R^2 = 0.94). In this case, the PLS modeling used only two principal components. This result indicates that for JFI, the PLS procedure was better than NN. The dimensionless parameter TFI/JFI yielded a better model with NN (R^2 = 0.87) compared with PLS modeling (R^2 = 0.80, 10 principal components). For HR, NN also yielded a better model (R^2 = 0.88) compared with 3D nonlinear modeling (R^2 = 0.60).

TABLE IV
Neural Network Modeling Output for Carr Compressibility (CC), Total Flowability Index (TFI), and Jenike Flow Index (JFI) with Multiple Input Single Output[a]

	CC			TFI			JFI		
Trial	R^2	MSE	CV (%)	R^2	MSE	CV (%)	R^2	MSE	CV (%)
1	0.35	10.39	24.60	0.59	14.72	4.98	0.68	1.44	27.42
2	0.78	5.33	16.99	0.69	11.74	4.17	0.62	0.94	22.72
3	0.47	9.99	21.22	0.38	6.48	2.19	0.58	7.92	19.80
4	0.55	10.18	30.23	0.55	4.89	2.41	**0.83**	**0.96**	**23.50**
5	0.69	6.22	14.84	0.34	6.47	2.88	0.70	0.84	21.83
6	0.56	6.35	16.99	0.50	5.41	2.51	0.51	1.22	24.57
7	0.64	7.63	19.91	0.44	5.85	2.58	0.44	1.32	28.38
8	0.66	7.66	23.43	0.03	7.32	2.87	0.58	1.31	31.66
9	0.67	7.96	22.43	0.34	6.39	2.76	0.56	1.29	29.02
10	0.65	9.44	20.46	0.40	6.39	2.68	0.63	0.97	27.95
11	0.78	6.94	19.12	0.36	6.81	2.80	0.73	1.14	26.96
12	0.59	10.14	21.20	0.71	3.77	2.11	0.72	1.05	31.34
13	0.68	6.77	17.55	0.75	3.05	1.73	0.79	0.68	27.18
14	0.55	8.92	19.62	0.65	4.12	2.17	0.57	1.52	35.31
15	0.68	5.45	16.36	0.64	4.05	1.94	0.12	3.62	54.19
16	0.63	5.04	15.74	0.76	3.10	1.78	0.62	1.07	27.09
17	0.73	6.01	18.53	0.76	3.07	1.68	0.68	0.97	22.67
18	0.63	6.07	19.54	0.67	3.98	2.11	0.57	1.26	26.23
19	0.32	9.25	21.68	0.59	4.84	2.17	0.75	0.70	24.59
20	0.62	7.63	16.47	0.09	5.41	2.31	0.57	1.16	32.75
21	0.74	4.40	13.79	0.13	5.87	2.49	0.51	1.26	26.61
22	0.62	8.85	24.02	0.55	3.75	1.91	0.50	1.57	27.20
23	0.58	9.41	20.40	0.80	2.46	1.63	0.12	2.38	32.00
24	0.68	4.97	16.16	0.79	2.24	1.51	0.54	1.31	26.36
25	0.74	6.03	15.11	0.86	1.40	1.23	0.56	1.12	25.71
26	**0.86**	**4.06**	**15.05**	**0.87**	**1.31**	**1.22**	0.61	1.18	23.92
27	0.63	8.01	21.94	0.84	1.56	1.32	0.53	1.33	26.20

[a] R^2 = coefficient of determination; MSE = mean square error; and CV = coefficient of variation. Bold font indicates that this neural network combination was best for modeling the response variable.

Model Validation

Another objective of this study was to validate the optimum NN models with external data, specifically that of Ganesan et al (2007), with moisture content as the independent variable (10, 15, 20, 25, and 30%, db). Table V represents the validation results using the Ganesan et al (2007) dataset. From Table V, HR (R^2 = 0.94, CV = 0.62%), ABD (R^2 = 0.83, CV = 3.32%), and CC (R^2 = 0.89, CV = 24.62%) validated the dataset of Ganesan et al (2007) with relatively high fit. JFI (R^2 = 0.63, CV = 27.36%) and TFI/JFI (R^2 = 0.63, CV = 24.51%), however, only yielded moderate fit,

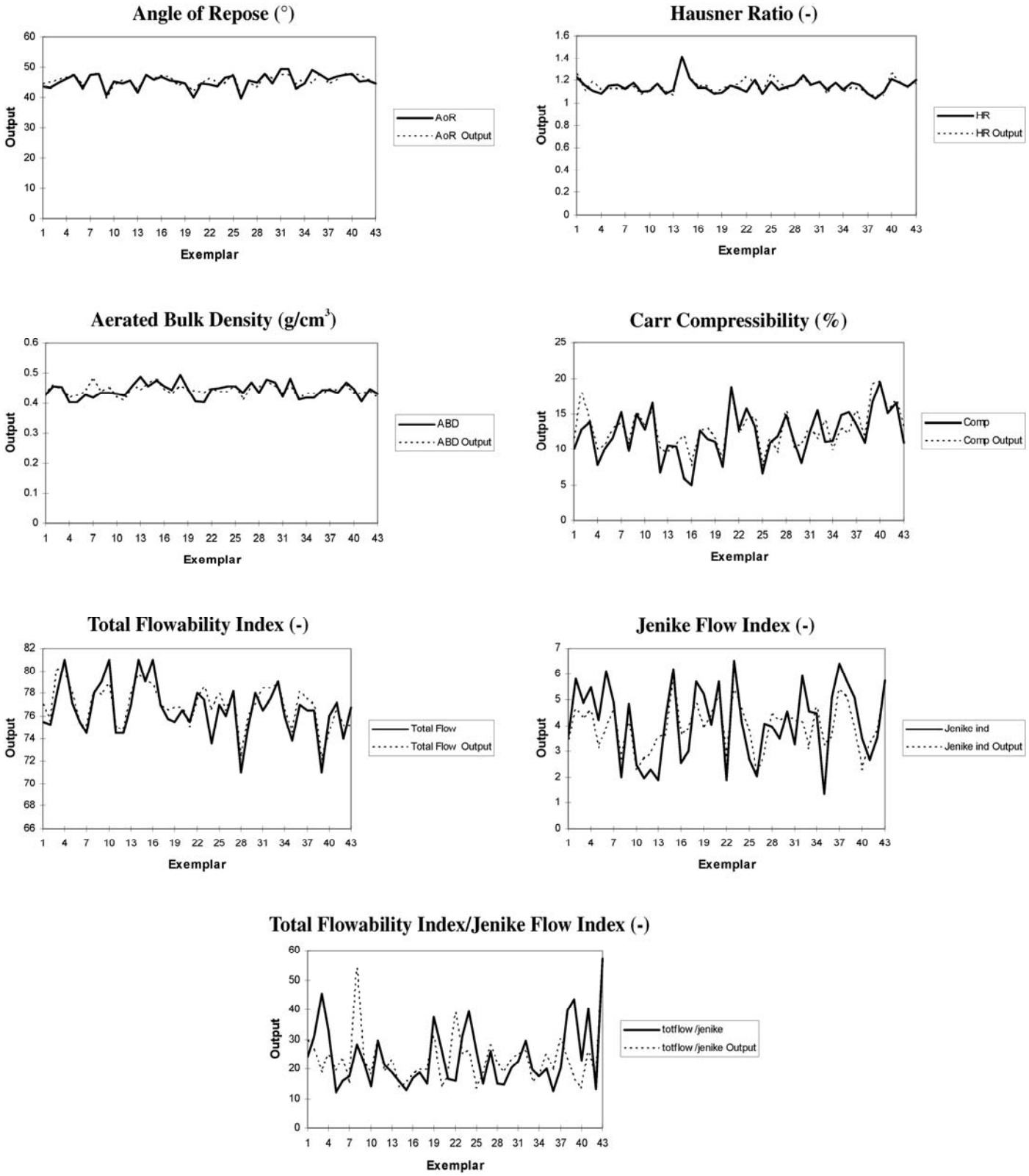

Fig. 1. Predicted output for flow properties using optimal neural network with condensed distillers solubles level (%, wb), drying temperature (°C), cooling temperature (°C), and storage time (months) as the independent variables. Exemplar was calculated as the total number of data points in the input set divided by the number of processing elements. Solid lines are observed output; dashed lines are predicted output.

indicating that the models did not do an excellent job of describing Ganesan et al (2007) data. However, AoR (R^2 = 0.38, CV = 3.56%) and TFI (R^2 = 0.29, CV = 2.47%) did not fit well, even though CV values were below 4%.

Figure 3 presents the predicted values for each response variable using the Ganesan et al (2007) data. Graphical representation also confirms that for AoR and TFI, there were wide differences between observed (solid line) and predicted (dashed line) values, indicating that our optimal NN models did not fit Ganesan et al (2007) data well. Ganesan et al (2007) data used moisture content as the independent variable and used 100 and 25°C for drying and cooling temperatures, respectively, throughout all experiments. So, possibly because of this difference in the number of input variables, there were some differences between predicted and observed values of AoR and TFI, as depicted in Figure 3.

Surface Plots of Predicted Flow Variables Obtained from the Optimal NN Models

In the last phase of this study, we graphically displayed the predicted values of each response variable obtained from the optimal NN models according to CDS level and C/D. Figure 4A gives the optimal predicted surface for AoR. For DDGS, a lower AoR, ≈42°, would indicate fair to passable flow behavior, but a higher AoR, ≈48°, would signify cohesive DDGS flow behavior (Carr 1965). Thus, according to the AoR prediction plot, it is clear that lower CDS levels (<13%, wb) combined with a 0.2–0.4 C/D would create DDGS with better flowability (AoR ≈42°). A C/D of

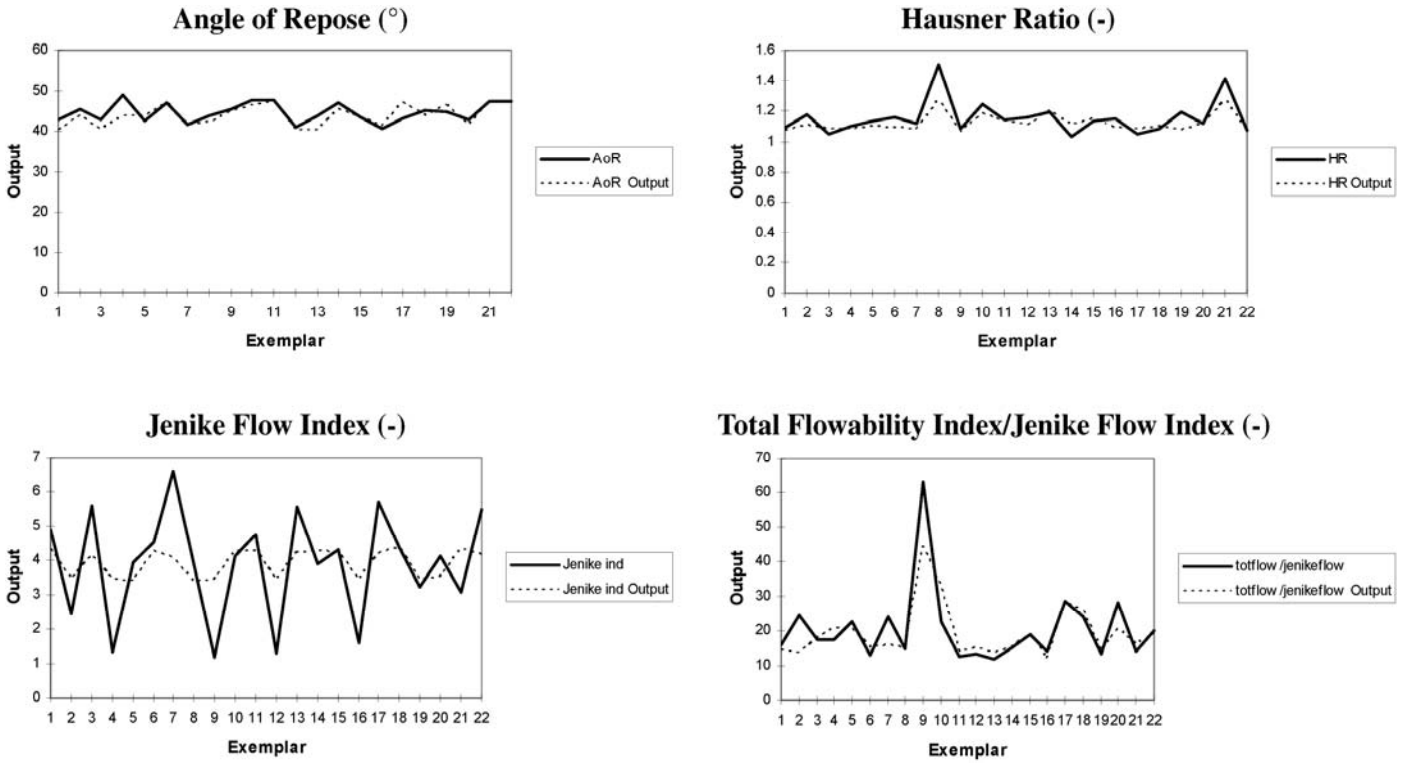

Fig. 2. Predicted output for flow properties for data obtained from Bhadra et al (2010a) using an artificial neural network with the optimal network structure indicated in Table V without storage time as an independent variable. Exemplar was calculated as the total number of data points in the input set divided by the number of processing elements. Solid lines are observed output; dashed lines are predicted output.

TABLE V
Comparison of Optimal Neural Networks (This Study) with Bhadra et al (2010a) Results and Model Validation with Ganesan et al (2007) Data for Key Flow Properties of DDGS[a]

	Optimal NN Models (with storage time included in independent variables)			Optimal NN Models (without storage time included in independent variables)			Modeling Results of Bhadra et al (2010a)		NN Modeling with Ganesan et al (2007) Data Set		
Response Variables	R^2	CV (%)	Optimal Structure	R^2	CV (%)	Optimal Structure	R^2	Optimal Structure	R^2	CV (%)	Optimal Structure
AoR (°)	0.87	2.16	Trial 16	0.89	3.14	Trial 16	0.89	9 components (PLS modeling)	0.38	3.56	Trial 16
JFI (-)	0.83	23.50	Trial 4	0.73	42.83	Trial 4	0.94	2 components (PLS modeling)	0.63	27.36	Trial 4
TFI/JFI (-)	0.65	26.15	Trial 26	0.87	14.81	Trial 4	0.80	10 components (PLS modeling)	0.63	24.51	Trial 4
HR (-)	0.84	2.30	Trial 26	0.88	4.08	Trial 26	0.60	0.06 SEM (3D modeling)	0.94	0.62	Trial 26
ABD (g/cm^3)	0.83	3.32	Trial 17	0.85	3.09	Trial 17			0.83	3.32	Trial 17
CC (%)	0.86	15.05	Trial 26	0.83	16.31	Trial 26			0.89	24.62	Trial 26
TFI (-)	0.87	1.22	Trial 26	0.89	1.16	Trial 26			0.29	2.47	Trial 26

[a] DDGS = distillers dried grains with solubles; NN = neural network; AoR = angle of repose; JFI = Jenike flow index; TFI = total flowability index; HR = Hausner ratio; ABD = aerated bulk density; CC = Carr compressibility; and SEM = standard error of the mean. For NN trial information, refer to Table II.

0.1 to –0.1, combined with a CDS level of ≈19% (wb), could create DDGS with potential flow problems (AoR ≈48°). For Ganesan et al (2008b), higher moisture content (>25%, db) showed some lubricating effects and slightly improved flow behavior. However, for our case, such lubricating effects at higher CDS levels were not seen, and the cohesive nature of DDGS increased with an increase in CDS levels. CDS is relatively high in fat content (6–12%, db) (Rosentrater and Muthukumarappan 2006). High CDS levels correlate to high fat levels in DDGS. Fat can be a major cause in cohesiveness between DDGS particles because temperature fluctuations (e.g., high summer temperatures) can lead to phase changes (e.g., partial melting, changes in crystallinity) of adjacent fat molecules and increase the cohesive strength between particles (Bhadra et al *in press* a).

Figure 4B presents the optimal HR plot according to CDS level and C/D. Higher HR (>1.15) generally indicates poor or cohesive flow in DDGS (Bhadra et al 2009b). However, according to Ganesan et al (2007), empirical modeling of DDGS predicted that for HR between 1.03 and 1.05, "fair" or potentially problematic flow would occur, but for HR > 1.05, "poor" flow or flow with definite problems would exist. From Figure 4B, we can see that lower CDS levels combined with 0.2–0.4 or –0.1 to –0.2 C/D yielded HR > 1.15, indicating potential flow problems in the DDGS.

According to Figure 4C, predicted ABD did not have much relationship to CDS level at levels greater than 13% (wb), but there was a marked increase in ABD with an increase in C/D. ABD may be related to particle size. Lower bulk densities (at CDS > 13% [wb] and C/D from 0.1 to 0.4) represent more entrapped void spaces resulting from larger particle sizes (Yan and Barbosa-Canovas 1997). Again, larger particle size would indicate a lower surface area to volume ratio, and thus, less cohesiveness and better flow (Farley and Valentin 1967).

Figure 4D shows the optimal CC modeling results and indicates that C/D had a major influence on CC, whereas CDS level did not. Lower CC (<15%) generally indicates good flow behavior in powders (Carr 1965), and in this case, C/D between 0.1 and –0.1 predicted DDGS with low CC and, hence, good flow.

Figure 4E gives the optimal predicted plot of TFI. TFI > 75 generally indicates good flow behavior, and index values be-

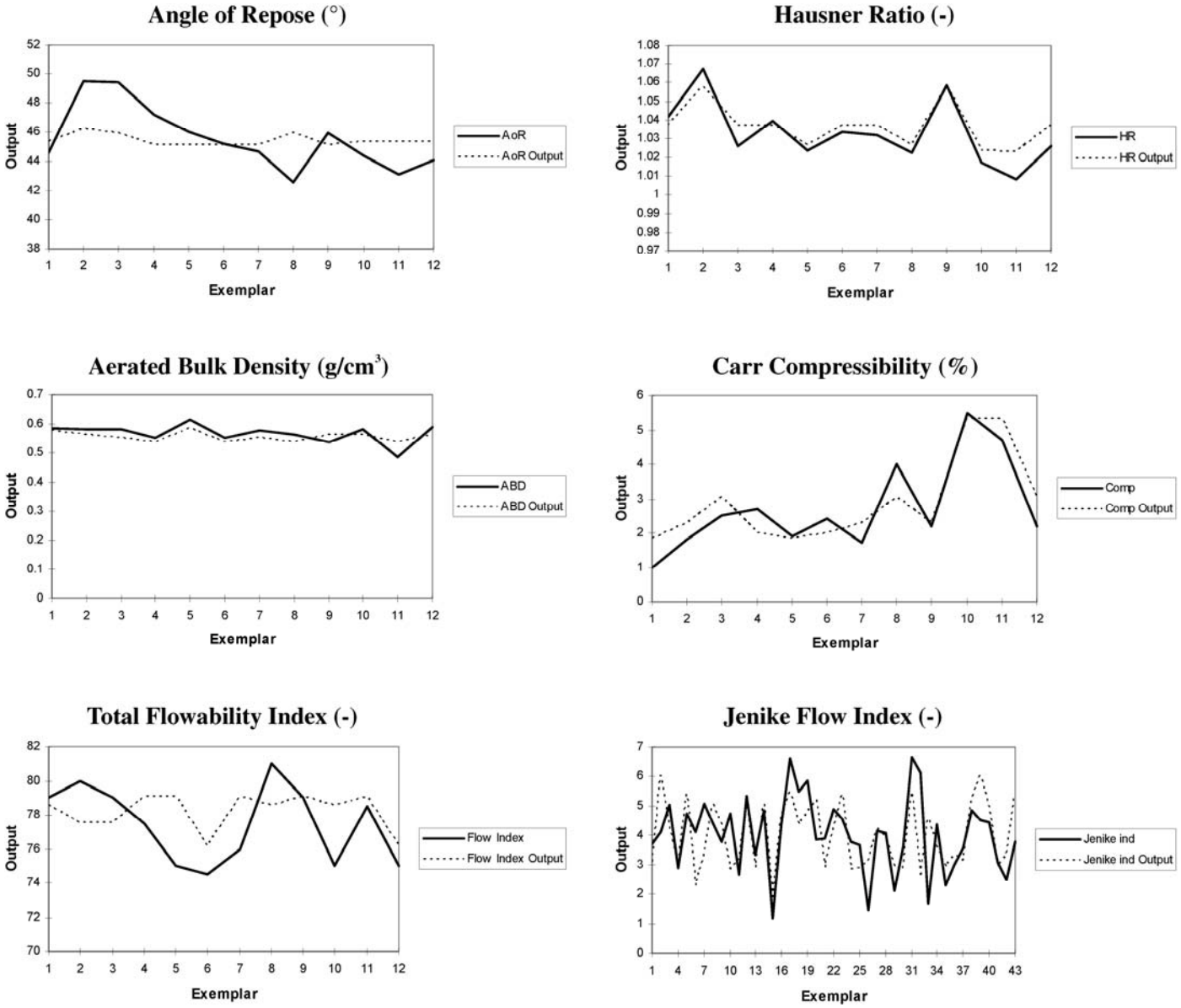

Fig. 3. Predicted output for flow properties for data obtained from Ganesan et al (2007) using an artificial neural network with the network structure indicated in Table V. Exemplar was calculated as the total number of data points in the input set divided by the number of processing elements. Solid lines are observed output; dashed lines are predicted output.

tween 60 and 75 indicate fair flow behavior in bulk solids (Carr 1965). According to Figure 4E, higher CDS levels (>18%, wb) combined with higher C/D (0.25–0.4) predict TFI values between 72 and 74, indicating some possible flow problems in the DDGS samples.

Figure 4F presents the optimal predicted JFI for varying CDS and C/D. JFI > 4 generally indicates fair to good flow behavior in bulk solids (Fitzpatrick et al 2004). From our predicted surface, we observe that CDS levels <17% (wb) combined with C/D in the range of 0.1 to –0.05 predict higher JFI (>4) for DDGS samples, hence indicating good flow behavior.

CONCLUSIONS

This research revealed that NN modeling was successful in predicting the behavior of key flow properties of DDGS as a function of multiple process (CDS addition level and drying temperature) and environmental or storage variables (cooling temperature and storage time) with only one hidden layer and employing MLP network architecture. For AoR, TFI/JFI, and HR, NN modeling yielded better models (R^2 > 0.87) than both PLS multivariate modeling and response surface modeling done in our previous studies. Our proposed NN models were validated with other

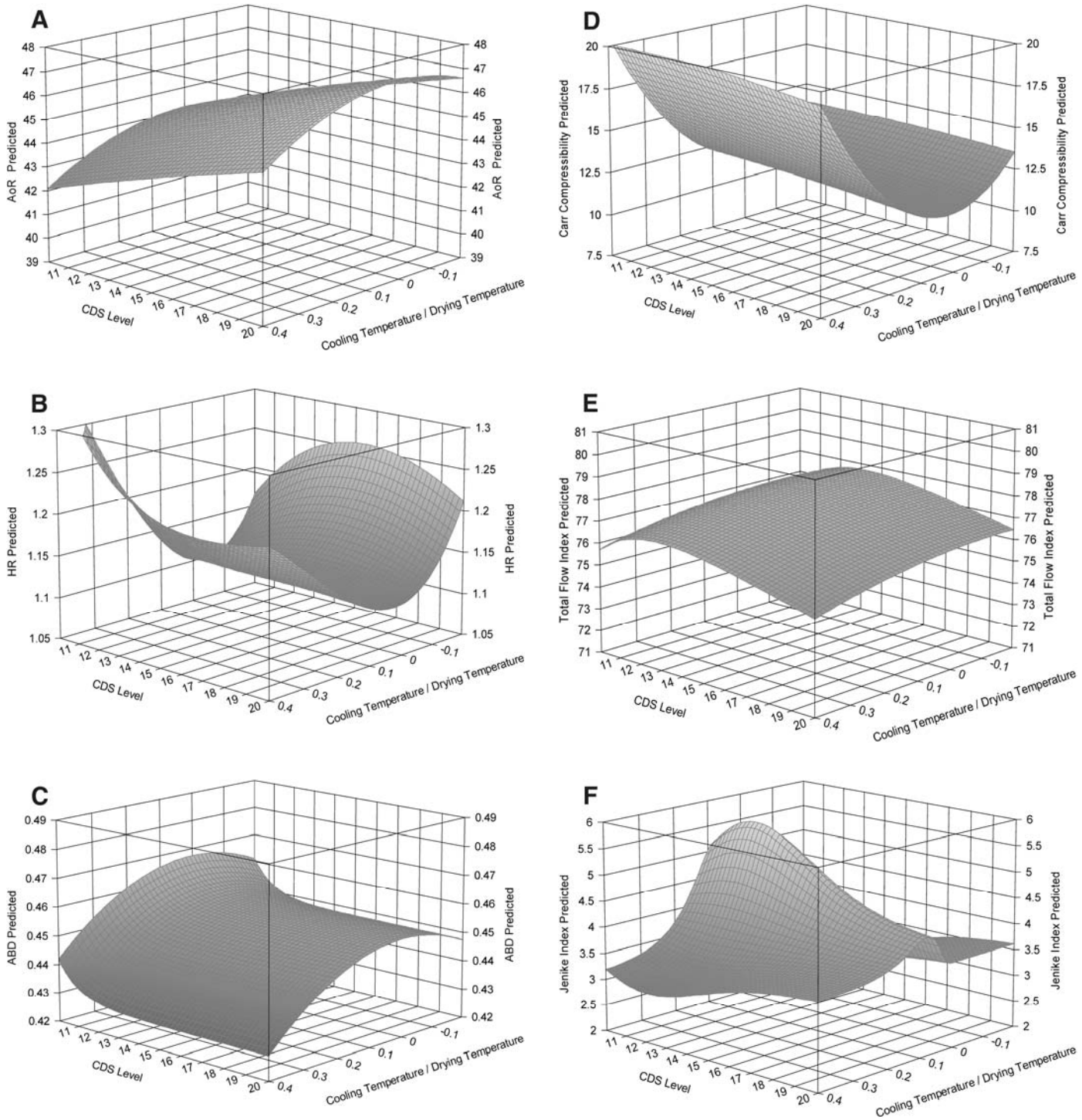

Fig. 4. Graphical representation of the predicted surfaces obtained from the optimal neural network model as a function of the ratio of cooling temperature to drying temperature (-) and condensed distillers solubles (CDS) level (%, wb). **A,** angle of repose (AoR, °); **B,** Hausner ratio (HR, -); **C,** aerated bulk density (ABD, g/cm^3); **D,** Carr compressibility (%); **E,** total flowability index (-); and **F,** Jenike flow index (-).

DDGS flowability data as well, with resulting model performance of $R^2 > 0.83$ for several variables, although not all of them. Observed and predicted plots were in accordance with the NN model performance values. From a practical point of view, this study was able to predict values for DDGS flow properties with respect to varying CDS, drying temperature, cooling temperature, and storage time levels. Hence, from the predicted plots, it was possible to classify flow properties (favorable or cohesive flow) based on given CDS levels and C/D.

Drying temperature and CDS levels were based on discussions with industry experts. Cooling temperature and storage time levels were selected to cover average ambient temperature and DDGS hauling times faced by the DDGS industry. The key points from these results are as follows.

CDS levels below 13% (wb) would produce DDGS with AoR ≈42°, low HR values, and JFI > 4, indicating noncohesive DDGS.

CDS levels up to 14% (wb) resulted in DDGS with the highest TFI values, indicating good DDGS flow characteristics.

Overall, AoR, HR, and JFI properties showed that C/D (-) values between 0.1 and –0.1 yielded DDGS with better flow behavior.

Thus, predicted surface plots can serve as a useful tool for industrial practice and academic research to predict the flow behavior of DDGS under given process and environmental conditions. Such predictive modeling encompasses a wide range of possible conditions in DDGS production. This approach could open new possibilities for applying artificial intelligence based algorithms toward understanding flowability of DDGS and other bulk solids.

ACKNOWLEDGMENTS

The authors would like to extend their gratitude to South Dakota State University and USDA-ARS for their financial support for this project. The authors would also like to extend appreciation to South Dakota Corn Utilization Council and Agricultural Experimental Station.

LITERATURE CITED

Agricultural Utilization Research Institute (AURI) and Minnesota Corn Growers Association (MCGA). 2005. Distiller's dried grains flowability report. Available at http://www.auri.org/research/Flowability_summary_10_17_05.pdf.

Baawain, M. S., El-din, M. G., and Smith, D. W. 2007. Artificial neural network modeling of ozone bubble columns: Mass transfer coefficient, gas hold-up, and bubble size. Ozone: Sci. Eng. 29:343-352.

Batchelor, W. D., Yang, X. B., and Tschanz, A. T. 1997. Development of a neural network for soybean rust epidemics. Trans. ASAE 40:247-252.

Bhadra, R., Muthukumarappan, K., and Rosentrater, K. A. 2009a. Flowability properties of commercial distillers dried grains with solubles (DDGS). Cereal Chem. 86:170-180.

Bhadra, R., Rosentrater, K. A., and Muthukumarappan, K. 2009b. Effects of CDS and drying temperature levels on the flowability behavior of DDGS. ASABE paper 095844. St. Joseph, MI.

Bhadra, R., Muthukumarappan, K., and Rosentrater, K. A. 2010a. Effects of varying CDS levels and drying and cooling temperatures on flowability properties of DDGS. ASABE paper 1008604. St. Joseph, MI.

Bhadra, R., Muthukumarappan, K., and Rosentrater, K. A. 2010b. Physical and chemical characterization of fuel ethanol coproducts relevant to value-added uses. Cereal Chem. 87:439-447.

Bhadra, R., Rosentrater, K. A., and Muthukumarappan, K. 2010c. Modeling DDGS flowability with varying drying and storage parameters. ASABE paper 1008715. St. Joseph, MI.

Bhadra, R., Rosentrater, K. A., and Muthukumarappan, K. *In press* a. Effects of varying CDS, drying and cooling temperatures on glass transition temperature of DDGS. Can. Biosyst. Eng.

Bhadra, R., Rosentrater, K. A., Muthukumarappan, K., and Kannadhason, S. *In press* b. Desorption studies of DDGS under varying CDS and drying temperature levels. Appl. Eng. Agric.

Boillereaux, L., Cadet, C., and Bail, A. L. 2003. Thermal properties estimation during thawing via real-time neural network learning. J. Food Eng. 57:17-23.

Carr, R. L., Jr. 1965. Evaluating flow properties of solids. Chem. Eng. 72:163-168.

Chevanan, N., Muthukumarappan, K., and Rosentrater, K. A. 2007. Neural network and regression modeling of extrusion processing parameters and properties of extrudates containing DDGS. Trans. ASABE 50:1765-1778.

Denicoff, M. R. 2007. Ethanol transportation backgrounder. Agricultural Marketing Service, USDA: Washington, DC. Available online at http://www.ams.usda.gov/AMSv1.0/getfile?dDocName=STELPRDC5063605.

Faqih, A., Chaudhuri, B., Alexander, A. W., Davies, C., Muzzio, F. J., and Tomassone, M. S. 2007. An experimental/computational approach for examining unconfined cohesive powder flow. Int. J. Pharm. 324:116-127.

Farley, R., and Valentin, F. H. H. 1967. Effect of particle size upon the strength of the powder. Powder Technol. 1:344-354.

Fitzpatrick, J. J., Iqbal, T., Delaney, C., Twomey, T., and Keogh, M. K. 2004. Effect of powder properties and storage conditions on the flowability of milk powders with different fat contents. J. Food Eng. 64:435-444.

Ganesan, V., Rosentrater, K. A., and Muthukumarappan, K. 2007. Modeling the flow properties of DDGS. Cereal Chem. 84:556-562.

Ganesan, V., Muthukumarappan, K., and Rosentrater, K. A. 2008a. Effect of moisture content and soluble level on the physical, chemical, and flow properties of distillers dried grains with solubles (DDGS). Cereal Chem. 85:464-470.

Ganesan, V., Muthukumarappan, K., and Rosentrater, K. A. 2008b. Flow properties of DDGS with varying soluble and moisture contents using Jenike shear testing. Powder Technol. 187:130-137.

Ganjyal, G., Hanna, M. A., Supprung, P., Noomhorm, A., and Jones, D. 2006. Modeling selected properties of extruded rice flour and rice starch by neural network and statistics. Cereal Chem. 83:223-227.

Ilari, J. L. 2002. Flow properties of industrial dairy powders (review). Le Lait 82:383-399.

Jenike, A. W. 1964. Storage and flow of solids. Utah Engineering Station bulletin 123. University of Utah: Salt Lake City, UT.

Kachrimanis, K., Karamyan, V., and Malamataris, S. 2003. Artificial neural networks and modeling of powder flow. Int. J. Pharma. 250: 13-23.

Knowlton, T. A., Carson, J. W., Klinzing, G. E., and Yang, W. C. 1994. The importance of storage, transfer, and collection. Chem. Eng. Prog. 90:44-54.

Linko, P., Zhu, Y. H., and Linko, S. 1992. Application of neural network modeling in fuzzy extrusion control. Food Bioprod. Process. 70:131-137.

Marini, F., Magri, A. L., and Bucci, R. 2007. Multilayered feed forward artificial neural network for class modeling. Chemom. Intell. Lab. Syst. 88:118-124.

McCarthy, J. J., and Ottino, J. M. 1998. Particle dynamics simulations: A hybrid technique applied to granular mixing. Powder Technol. 97: 91-99.

McCarthy, J. J., Vargas, W. L., and. Abatan, A. A. 2001. Discrete characterization tools for cohesive granular material. Powder Technol. 97:214-223.

Mikami, T., Kamiya, H., and Horio, M. 1998. Numerical simulation of cohesive powder behavior in a fluidized bed. Chem. Eng. Sci. 53:1927-1940.

Ochoa-Martinez, C. I., Ramaswany, H. S., and Ayala-Aponte, A. A. 2007. Artificial neural network modeling of osmotic dehydration mass transfer kinetics of fruits. Drying Technol. 25:85-95.

Olajos, M., Chovan, T., Mittermayr, S., Kenesei, T., Hojas, P., Molnar, I., Darvas, F., and Guttman, A. 2008. Artificial neural network modeling of pH dependent structural descriptor-mobility relationships for capillary zone electrophoresis of tripeptides. J. Liq. Chromatogr. Relat. Technol. 31:2348-2362.

Renewable Fuels Association (RFA). 2010. Industry resources coproducts. Available at www.ethanolrfa.org/industry/reseources/coproducts/. Accessed on March 12, 2010.

Riahi, S., Mousavi, M. F., Ganjal, M. R., and Norouzi, P. 2008. Application of correlation ranking procedure and artificial neural network in the modeling of liquid chromatographic retention times of various pesticides. Anal. Lett. 41:3364-3385.

Rosentrater, K. A., and Muthukumarappan, K. 2006. Corn ethanol coproducts: Generation, properties, and future prospects. Int. Sugar J. 108:648-657.

Santomaso, A., Lazzaro, P., and Canu, P. 2003. Powder flowability and density ratios: The impact of granules packing. Chem. Eng. Sci. 58:2857-2874.

Sofu, A., and Ekinci, F. Y. 2007. Estimation of storage time of yoghurt with artificial neural network. J. Dairy Sci. 90:3118-3125.

Torrecilla, J. S., Otero, L., and Sanz, P. D. 2005. Artificial neural networks: A promising tool to design and optimize high pressure food processes. J. Food Eng. 69:299-306.

Wier, G. J. 2004. A mathematical model for dilating, non-cohesive granular flows in steep-walled hoppers. Chem. Eng. Sci. 59:149-161.

Yan, H., and Barbosa-Canovas, G. V. 1997. Compression characteristics of agglomerated food powders: Effect of agglomerate size and water activity. Food Sci. Technol. Int. 3:351-359.

Yang, S. C., and Hsiau, S. S. 2001. The simulation of powders with liquid bridges in a 2D vibrated bed. Chem. Eng. Sci. 56:6837-6849.

[Received December 28, 2010. Accepted August 4, 2011.]